Enhanced Negative Thermal Expansion in La$_{1-x}$Pr$_x$Fe$_{10.7}$Co$_{0.8}$Si$_{1.5}$ Compounds by Doping the Magnetic Rare-Earth Element Praseodymium

Wen Li,[†,‡] Rongjin Huang,*,[†] Wei Wang,[†] Jie Tan,[†,‡] Yuqiang Zhao,[†,‡] Shaopeng Li,[†,‡] Chuanjun Huang,[†] Jun Shen,[†] and Laifeng Li*,[†]

[†]Key Laboratory of Cryogenics, Technical Institute of Physics and Chemistry, Chinese Academy of Sciences, Beijing, P. R. China
[‡]University of Chinese Academy of Sciences, Beijing, P. R. China

ⓢ *Supporting Information*

ABSTRACT: Experiments have been performed to enhance negative thermal expansion (NTE) in the La(Fe,Co,Si)$_{13}$-based compounds by optimizing the chemical composition, i.e., proper substitution of La by magnetic element Pr. It is found that increasing the absolute value of the average coefficient of thermal expansion (CTE) in the NTE temperature region (200−300 K) attributes to enhancement of the spontaneous magnetization and its growth rate with increasing Pr content. Typically, the average CTE of La$_{1-x}$Pr$_x$Fe$_{10.7}$Co$_{0.8}$Si$_{1.5}$ with x = 0.5 reaches as large as −38.5 × 10^{-6} K^{-1} between 200 and 300 K (ΔT = 100 K), which is 18.5% larger than that of x = 0. The present results highlight the potential applications of La(Fe,Co,Si)$_{13}$-based compounds with a larger NTE coefficient.
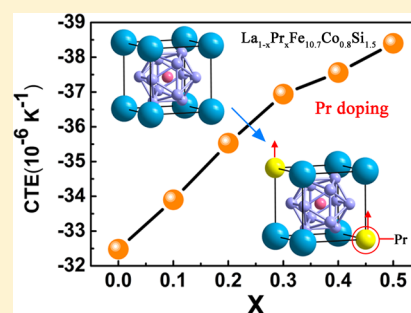
1. INTRODUCTION

Negative thermal expansion (NTE) materials contract when heated rather than expand as most materials do. In recent years, many studies have been conducted on the NTE materials because of their potential applications for high precision devices, such as optical mirrors, fiber-optic systems, and electrooptical sensors, in which it is necessary to compensate for the normal positive thermal expansion. Up to now, several kinds of materials with NTE properties were discovered, such as LiAlSiO$_4$ (β-eucryptite), ZrW$_2$O$_8$,[1,2] ReO$_3$,[3] CuO nano-particles,[4] ScF$_3$,[5,6] PbTio$_3$-based compounds,[7] La(Fe,Si)$_{13}$-based compounds,[8] and antiperovskite manganese nitride.[9−15] It is noteworthy, however, that only a very limited number of NTE materials serve as thermal volume-expansion compensators in practical applications because of the relatively narrow NTE operation-temperature window, low NTE coefficient, thermal expansion anisotropy, and low mechanical strength and electrical conductivity.[8] Among these NTE materials, La-(Fe,Si)$_{13}$-based compounds have been recently developed as promising NTE materials, which show large, isotropic, and nonhysteretic NTE properties and relatively high electrical and thermal conductivities.

The NTE property of the La(Fe,Si)$_{13}$-based compounds originates from a large magnetovolume effect (MVE), which counteracts or is even larger than the normal thermal expansion. In the NaZn$_{13}$-type crystal structure La(Fe,Si)$_{13}$-based compounds, Fe atoms occupy two nonequivalent sites, 8b (Fe^I) and 96i (Fe^{II}), respectively. The Fe^I atom is surrounded by an icosahedron with 12 Fe^{II} atoms, while the Fe^{II} atom has 1 Fe^I atom and 9 Fe^{II} atoms as the nearest neighbors.[16,17] The Fe^I−Fe^{II} distance plays a critical role in the

exchange interaction of energy. Hence, the change of the Fe^I−Fe^{II} distance due to substitutional or interstitial addition will affect the magnetic moments and thus alter the thermal expansion properties. It has been revealed that the NTE operation-temperature window can be varied by raising the magnetic transition temperature when Fe is partially substituted by other elements,[8] which makes it more useful for practical applications in different temperature ranges. For instance, in the previous work, the experimental results indicate that the NTE operation-temperature window of LaFe$_{11.5-x}$Co$_x$Si$_{1.5}$ can be tuned to room temperature by the partial substitution of Co for Fe.[8] The crystal structure is shown in Figure 1. On the other hand, an increase of the NTE coefficient will provide remarkable improvement with respect to compensating for the usual positive thermal expansion of materials with a higher CTE, such as polymers. In this report, discussion will be done about whether the NTE coefficient of the La(Fe,Si)$_{13}$-based compounds can be further improved by increasing the magnetic moments when La is partially substituted by appropriate magnetic elements.

An investigation was performed on the effect of enhancement of magnetic moments on the NTE coefficient in the La(Fe,Co,Si)$_{13}$-based compounds with the proper substitution of magnetic element Pr for La. It was discovered that the NTE coefficient indeed increases with higher Pr content because of the enlarged magnetic moments.
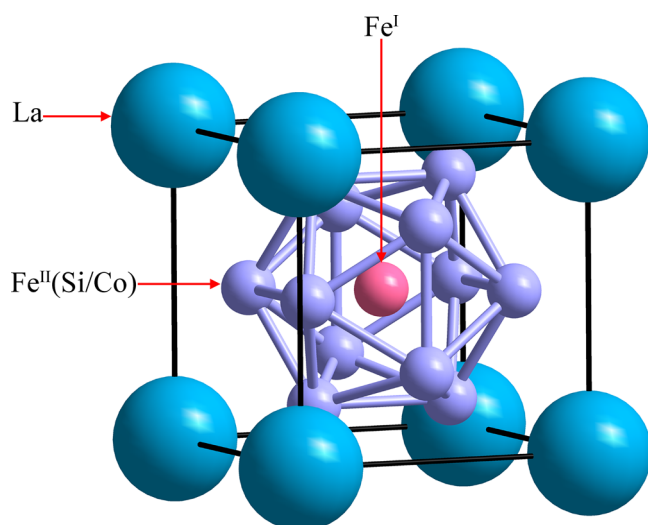
Figure 1. NaZn$_{13}$-type structure (space group $Fm\overline{3}c$) of the La(Fe,Co,Si)$_{13}$-based compounds.

2. EXPERIMENTAL INFORMATION

Polycrystalline samples of La$_{1-x}$Pr$_x$Fe$_{10.7}$Co$_{0.8}$Si$_{1.5}$ (x = 0, 0.1, 0.2, 0.3, 0.4, 0.5, and 0.6) were prepared in an arc-melting furnace under a high-purity argon atmosphere. The raw materials of La, Fe, Co, Si, and Pr were at least 99.9% pure. Button samples were melted four times, and each time the buttons were flipped to ensure homogeneity during melting. The arc-melted ingots wrapped by Ta foils were sealed in a quartz tube filled with high-purity argon gas, subsequently homogenized at 1100 °C for 40 days, and finally quenched quickly into ice water.

In situ powder X-ray diffraction (XRD) was employed to identify the phase purity and crystal structure at different temperatures. The patterns were analyzed by JADE, using a cubic ($Fm\overline{3}c$) model.[18,19]

The linear thermal expansion data ($\Delta L/L_{300 K}$) were measured by using a strain gauge over a temperature range of 77−350 K. (Note that, for sintered polycrystalline samples, $\Delta L/L$ is related directly to the volume expansion in a manner of $\Delta L/L = \Delta V/3V$.) Measurement

of the linear thermal expansion in this way requires a reference material with known thermal expansion [ZERODUR glass ceramic, whose coefficient of thermal expansion (CTE) is nearly zero].

The magnetic properties were measured by means of a physical property measurement system.

3. RESULTS AND DISCUSSION

Phase Purity and Crystal Structure. Figure 2a shows the X-ray patterns of the tested family of La$_{1-x}$Pr$_x$Fe$_{10.7}$Co$_{0.8}$Si$_{1.5}$ (x = 0, 0.1, 0.2, 0.3, 0.4, 0.5, and 0.6) at room temperature. The indices of the crystallographic plane (hkl) of reflections are shown in the figure. It indicates that these samples have a dominating phase with the NaZn$_{13}$-type structure. There are no visible diffraction peaks of pure elements or other second phases in the XRD patterns, except for the sample of La$_{1-x}$Pr$_x$Fe$_{10.7}$Co$_{0.8}$Si$_{1.5}$ with x = 0.6. A small amount of α-Fe is detected, as marked by the symbol ▼. This confirms that a Pr content of more than x = 0.5 could lead to the appearance of the α-Fe phase and be unfavorable for formation of the cubic NaZn$_{13}$-type structure. Therefore, the thermal expansion and magnetic properties of La$_{1-x}$Pr$_x$Fe$_{10.7}$Co$_{0.8}$Si$_{1.5}$ with x = 0.6 will not be discussed in this paper. Variation in the lattice parameters with increasing Pr content is shown in Figure 2b. It is obvious that the lattice parameter (a = 1.1484, 1.1479, 1.1442, 1.1437, 1.1430, and 1.1428) decreases with increasing Pr content; i.e., the partial substitution of Pr for La leads to contraction of the lattice. This result can be well determine that the Pr atom is smaller than the La atom. Figure 2c shows the XRD patterns of the (422) peak for La$_{0.5}$Pr$_{0.5}$Fe$_{10.7}$Co$_{0.8}$Si$_{1.5}$ at different temperatures. We learned that it maintains the cubic NaZn$_{13}$-type structure in the whole temperature range examined. Also, the reflections are shifted slightly to lower 2θ angles with decreasing test temperatures, which means that the lattice parameter increases with decreasing temperature and, consequently, its volume expands.

Thermal Expansion Properties. Figure 3 displays linear thermal expansion ($\Delta L/L$) data (reference temperature: 300
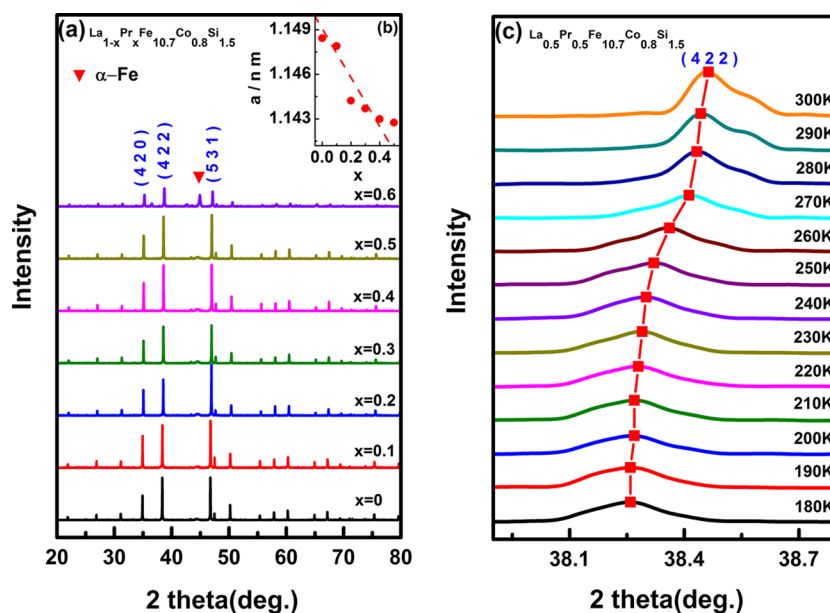

Figure 2. (a) XRD patterns for samples of La$_{1-x}$Pr$_x$Fe$_{10.7}$Co$_{0.8}$Si$_{1.5}$ (x = 0, 0.1, 0.2, 0.3, 0.4, 0.5, and 0.6) at room temperature. (b) Crystal lattice parameters as a function of the Pr concentration for samples of La$_{1-x}$Pr$_x$Fe$_{10.7}$Co$_{0.8}$Si$_{1.5}$ (x = 0, 0.1, 0.2, 0.3, 0.4, and 0.5) at room temperature. (c) XRD patterns of the (422) peak for La$_{1-x}$Pr$_x$Fe$_{10.7}$Co$_{0.8}$Si$_{1.5}$ with x = 0.5 at different temperatures.

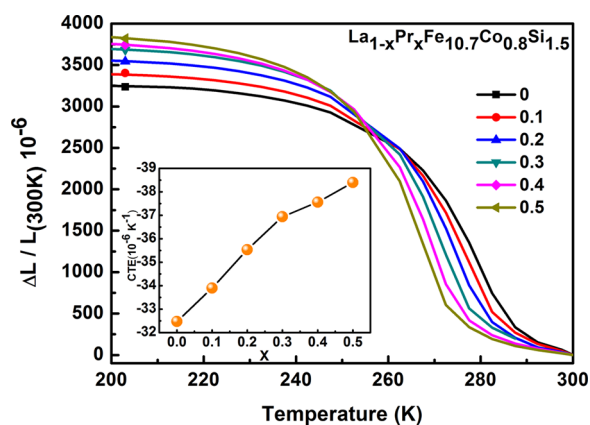**Figure 3.** Temperature dependence of linear thermal expansion $\Delta L/L$ (reference temperature: 300 K) for samples of $La_{1-x}Pr_xFe_{10.7}Co_{0.8}Si_{1.5}$ (x = 0, 0.1, 0.2, 0.3, 0.4, and 0.5). The inset shows the average CTE between 200 and 300 K as a function of the Pr concentration.

K) as a function of the temperature of $La_{1-x}Pr_xFe_{10.7}Co_{0.8}Si_{1.5}$ (x = 0, 0.1, 0.2, 0.3, 0.4, and 0.5). For each sample, $\Delta L/L$ rises with decreasing temperature in the whole temperature range examined. Specifically, $\Delta L/L$ grows gradually around room temperature, then increases rapidly, and again grows slowly with decreasing temperature, indicating that NTE occurs in the whole range measured (200−300 K). It is worth noting that the $\Delta L/L$ versus T curves are different from one another, which demonstrates that the NTE properties are affected by the partial substitution of La by Pr. From the $\Delta L/L$ versus T curves, we can calculate the average CTE, defined as $[(\Delta L/L)_{T_2} - (\Delta L/L)_{T_1}]/(T_2 - T_1)$. With an increase in the amount of Pr from x = 0.0 to 0.5, the absolute value of the average CTE (200−300 K) is enhanced with increasing Pr content, as shown in the inset of Figure 3. For example, without the partial substitution of La, $La_{1-x}Pr_xFe_{10.7}Co_{0.8}Si_{1.5}$ with x = 0 shows an average CTE of -32.5×10^{-6} K^{-1} between 200 and 300 K (ΔT = 100 K), whereas for $La_{1-x}Pr_xFe_{10.7}Co_{0.8}Si_{1.5}$ with x = 0.1 and 0.3, the average CTEs are -33.8×10^{-6} and -36.8×10^{-6} K^{-1}, respectively. In particular, the average CTE of $La_{1-x}Pr_xFe_{10.7}Co_{0.8}Si_{1.5}$ with x = 0.5 reaches as large as -38.5×10^{-6} K^{-1}, which is 18.5% larger than that of x = 0. Moreover, the absolute value of the average CTE in the temperature region where $\Delta L/L$ increases rapidly with decreasing temperature was also calculated. The CTEs are -77.9×10^{-6}, -78.3×10^{-6}, -80.0×10^{-6}, -80.6×10^{-6}, -80.8×10^{-6}, and -80.9×10^{-6} K^{-1} from x = 0.0 to 0.5.

Magnetic Properties. Considering that the NTE behavior is triggered by magnetic transition, an investigation of the magnetic properties would be very helpful for elucidating the underlying mechanisms of the NTE properties. The temperature dependence (200−350 K) of the magnetization $M(T)$ of all samples measured in a magnetic field of 100 Oe is shown in Figure 4a. The $M(T)$ curve exhibits a sharp ferromagnetic−paramagnetic (FM−PM) phase transition. The Curie temperatures (T_C) were determined from dM/dT curves, leading to the values of 290, 285, 282, 280, 277, and 275 K for $La_{1-x}Pr_xFe_{10.7}Co_{0.8}Si_{1.5}$ (x = 0, 0.1, 0.2, 0.3, 0.4, and 0.5), respectively. It is obvious that T_c is linearly dependent on the Pr content. Investigations on the relationship between the unit-cell volume and Curie temperature for the $La_{1-x}Pr_xFe_{10.7}Co_{0.8}Si_{1.5}$ compounds have verified that expanding the lattice can cause T_C to increase, while compressing the lattice can cause T_C to
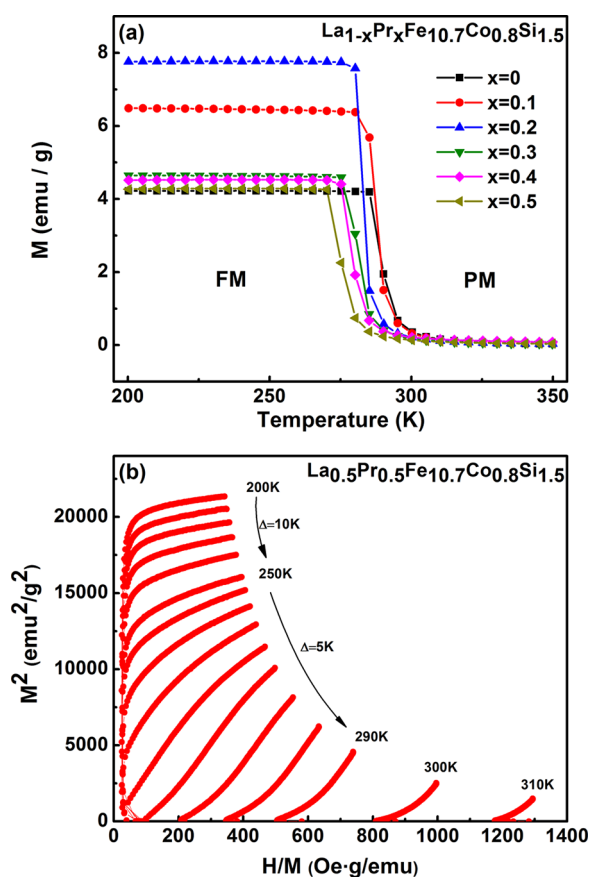

Figure 4. (a) Temperature dependence of magnetization in a magnetic field of 0.01 T for samples of $La_{1-x}Pr_xFe_{10.7}Co_{0.8}Si_{1.5}$ (x = 0, 0.1, 0.2, 0.3, 0.4, and 0.5). (b) Arrott plots of $La_{1-x}Pr_xFe_{10.7}Co_{0.8}Si_{1.5}$ with x = 0.5.

decrease.[20] This small reduction of T_C attributed to the lattice contraction is introduced by the partial substitution of La by Pr (Figure 2b), as reported in the literature.[20]

In order to obtain spontaneous magnetization, the isothermal magnetization versus applied field $M(H)$ were measured at different temperatures. Figure 4b exemplifies the typical Arrott plots derived from $M(H)$ within a broad temperature range around T_C for x = 0.5, with the temperature step of 5 K near T_C and 10 K apart from T_C. It is evident that the slope of the H/M versus M^2 curves is positive at all measured temperatures, which indicates that the phase transition is second-order according to the Banerjee criterion.[21] It is obvious that an inflection point in the Arrott plot at T_C is the signature of the itinerant electron magnetic transition from PM to FM order above T_C.[22] The spontaneous magnetization is deduced from the Arrott plots below T_C by extrapolating the Arrott plots to H/M = 0. Figure 5 displays spontaneous magnetization as a function of the temperature (200−270 K) for all samples. The spontaneous magnetization increases with a decrease of the temperature, and the rising rate became larger with increasing Pr content. It can be seen that spontaneous magnetization of $La_{1-x}Pr_xFe_{10.7}Co_{0.8}Si_{1.5}$ (x = 0.1, 0.2, 0.3, 0.4, and 0.5) is larger than that of $LaFe_{10.7}Co_{0.8}Si_{1.5}$ in the temperature range below T = 253 K and is smaller above T = 253 K. Jia et al.'s research has indicated that the magnetic moments grow with the increasing content of Pr.[23] As mentioned above, the NTE in $LaFe_{13-x}Si_x$-based compounds is due to the MVE accompanied by the change of magnetic ordering, which is responsible for
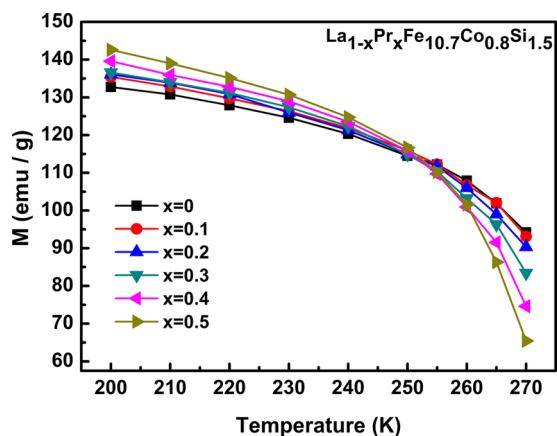
Figure 5. Spontaneous magnetization as a function of the temperature for samples of $La_{1-x}Pr_xFe_{10.7}Co_{0.8}Si_{1.5}$ (x = 0, 0.1, 0.2, 0.3, 0.4, and 0.5) below the Curie temperature.

contraction of the lattice parameter upon heating. In the following, consideration of the relationship between spontaneous magnetization and the NTE properties will be made. It can be seen from Figures 3 and 5 that the NTE behavior seems to synchronize with spontaneous magnetization; i.e., higher spontaneous magnetization corresponds to larger values of $\Delta L/L$ at the same temperature. This result has proven that the increase of spontaneous magnetization and its growth rate leads to larger expansion of the unit-cell volume with an increase of the Pr content.

It is well-known that the magnetic properties of rare-earth (R = La and Pr) transition-metal (T = Fe and Co) compounds are determined by the T−T, R−T, and R−R interactions. In general, the T−T interaction is the strongest; on the contrary, the R−R exchange is the weakest. In the host material $LaFe_{10.7}Co_{0.8}Si_{1.5}$, the magnetic properties are dependent on the Fe−Fe and Fe−Co interactions because of the nonmagnetic character of La. After introduction of the magnetic rare-earth element Pr, the Fe−Fe distance tends to weaken the exchange interactions among Fe atoms by increasing the overlap of Fe 3d wave functions.[24] However, the incorporation of magnetic element Pr could bring in a magnetic coupling between Pr and Fe, which would induce growth of the magnetic moment.[25] It was reported that, in $La_{1-x}Pr_xFe_{10.7}Co_{0.8}Si_{1.5}$, the magnetic moment increases linearly with an increase of the Pr content. It is estimated that the average magnetic moment per Pr atom is about 3.8 μ_B, which is close to the value of a free Pr^{3+} ion (3.5 μ_B).[20] What is more, the Pr atom is smaller than the La atom, which leads to smaller lattice parameters in the $La_{1-x}Pr_xFe_{10.7}Co_{0.8}Si_{1.5}$ compounds. Because this material exhibits NTE behavior when the spontaneous magnetic contribution overcomes the ordinary lattice thermal expansion, the prominent NTE means that there is large spontaneous magnetization in the $La_{1-x}Pr_xFe_{10.7}Co_{0.8}Si_{1.5}$ compounds.

4. CONCLUSIONS

In conclusion, we have investigated the effect of the enhancement of magnetic moments on the NTE coefficients in the $La(Fe,Co,Si)_{13}$-based compounds with the proper substitutions of Pr for La. The absolute value of the average CTE in the NTE temperature region adds linearly with increasing Pr content due to optimization of the chemical composition. Especially, the average CTE of $La_{1-x}Pr_xFe_{10.7}Co_{0.8}Si_{1.5}$ with x = 0.5 reaches as large as −38.5

$\times 10^{-6}$ K^{-1} between 200 and 300 K (ΔT = 100 K), which is 18.5% larger than that of x = 0. Consequently, we believe that the studied $La(Fe,Co,Si)_{13}$-based compounds with the proper substitutions of Pr for La are some of the most promising NTE materials for compensating for the more common positive thermal expansion that most materials have, especially some with a higher CTE.

■ ASSOCIATED CONTENT

Ⓢ Supporting Information

Temperature dependence of linear thermal expansion $\Delta L/L$ from 77 to 350 K (reference temperature: 300 K) for samples of $La_{1-x}Pr_xFe_{10.7}Co_{0.8}Si_{1.5}$ (x = 0, 0.1, 0.2, 0.3, 0.4, and 0.5). This material is available free of charge via the Internet at http://pubs.acs.org.

■ AUTHOR INFORMATION

Corresponding Authors
*E-mail: huangrongjin@mail.ipc.ac.cn.
*E-mail: laifengli@mail.ipc.ac.cn.
Notes
The authors declare no competing financial interest.

■ ACKNOWLEDGMENTS

■ REFERENCES

(1) Mary, T. A.; Evans, J. S. O.; Vogt, T.; Sleight, A. W. *Science* **1996**, *272*, 90−92.
(2) Perottoni, C. A.; Jornada, J. A. H. *Science* **1998**, *280*, 886−889.
(3) Chatterji, T.; Hansen, T. C.; Brunelli, M.; Henry, P. F. *Appl. Phys. Lett.* **2009**, *94*, 241902−3.
(4) Zheng, X. G.; Kubozono, H.; Yamada, H.; Kato, K.; Ishiwata, Y.; Xu, C. N. *Nat. Nanotechnol.* **2008**, *3*, 724−726.
(5) Li, C. W.; Tang, X. L.; Muñoz, J. A.; Keith, J. B.; Tracy, S. J.; Abernathy, D. L.; Fultz, B. *Phys. Rev. Lett.* **2011**, *107*, 195504.
(6) Greve, B. K.; Martin, K. L.; Lee, P. L.; Chupas, P. J.; Chapman, K. W.; Wilkinson, A. P. *J. Am. Chem. Soc.* **2010**, *132*, 15496−15498.
(7) Chen, J.; Nittala, K.; Forrester, J. S.; Jones, J. L.; Deng, J. X.; Yu, R. B.; Xing, X. R. *J. Am. Chem. Soc.* **2011**, *133*, 11114−11117.
(8) Huang, R. J.; Liu, Y. Y.; Fan, W.; Tan, J.; Xiao, F. R.; Qian, L. H.; Li, L. F. *J. Am. Chem. Soc.* **2013**, *135*, 11469−11472.
(9) Takenaka, K.; Takagi, H. *Appl. Phys. Lett.* **2005**, *87*, 261902.
(10) Sun, Y.; Wang, C.; Wen, Y. C.; Zhu, K. G.; Zhao, J. T. *Appl. Phys. Lett.* **2007**, *91*, 231913.
(11) Sun, Y.; Wang, C.; Huang, Q. Z.; Guo, Y. F.; Chu, L. H.; Arai, M.; Yamaura, K. *Inorg. Chem.* **2012**, *51*, 7232−7236.
(12) Song, X. Y.; Sun, Z. H.; Huang, Q. Z.; Rettenmayr, M.; Liu, X. M.; Seyring, M.; Li, G. N.; Rao, G. H.; Yin, F. X. *Adv. Mater.* **2011**, *23*, 4690−4694.
(13) Qu, B. Y.; Pan, B. C. *J. Appl. Phys.* **2010**, *108*, 113920.
(14) Lin, J. C.; Wang, B. S.; Lin, S.; Tong, P.; Lu, W. J.; Zhang, L.; Song, W. H.; Sun, Y. P. *J. Appl. Phys.* **2012**, *111*, 043905.
(15) Tong, P.; Louca, D.; King, G.; Llobet, A.; Lin, J. C.; Sun, Y. P. *Appl. Phys. Lett.* **2013**, *102*, 041908.
(16) Wang, F.; Wang, G. J.; Hu, F. X.; Kurbakov, A.; Shen, B. G.; Cheng, Z. H. *J. Phys.: Condens. Matter* **2003**, *15*, 5269.
(17) Wang, G. J.; Wang, F.; Di, N. L.; Shen, B. G.; Cheng, Z. H. *J. Magn. Magn. Mater.* **2006**, *303*, 84−91.

(18) Morelock, C. R.; Gallington, L. C.; Wilkinson, A. P. *Chem. Mater.* **2014**, *26*, 1936−1940.

(19) Carey, T.; Tang, C. C.; Hriljac, J. A.; Anderson, P. A. *Chem. Mater.* **2014**, *26*, 1561−1566.

(20) Shen, J.; Gao, B.; Dong, Q. Y.; Li, Y. X.; Hu, F. X.; Sun, J. R.; Shen, B. G. *J. Phys. D: Appl. Phys.* **2008**, *41*, 245005.

(21) Banerjee, S. K. *Phys. Lett.* **1964**, *12*, 16−17.

(22) Shen, J.; Li, Y. X.; Zhang, J.; Gao, B.; Hu, F. X.; Zhang, H. W.; Chen, Y. Z.; Rong, C. B.; Sun, J. R. *J. Appl. Phys.* **2008**, *103*, 07B317.

(23) Jia, L.; Sun, J. R.; Shen, J.; Dong, Q. Y.; Zou, J. D.; Gao, B.; Zhao, T. Y.; Zhang, H. W.; Hu, F. X.; Shen, B. G. *J. Appl. Phys.* **2009**, *105*, 07A924.

(24) Zhao, J. L.; Shen, J.; Hu, F. X.; Li, Y. X.; Sun, J. R.; Shen, B. G. *J. Appl. Phys.* **2010**, *107*, 113911.

(25) Jia, L.; Sun, J. R.; Shen, J.; Dong, Q. Y.; Hu, F. X.; Zhao, T. Y.; Shen, B. G. *Appl. Phys. Lett.* **2008**, *92*, 182503.

5873

dx.doi.org/10.1021/ic500801b | *Inorg. Chem.* 2014, 53, 5869−5873